

Effect of the Externally Seeded Impurities on Edge Localized Modes and Pedestal turbulence

G.L. Xiao¹, X.L. Zou², W.L. Zhong¹, M. Xu¹, Y.P. Zhang¹, D. Mazon², C.F. Dong¹, J.Q. Dong^{1,3}, K.R. Fang¹, B.B. Feng¹, J.M. Gao¹, M.K. Han^{1,4}, X.X. He¹, J. Li^{1,4}, Y.G. Li¹, A.S. Liang¹, X.M. Song¹, Z.B. Shi¹, P. Sun¹, J. Wen¹, Z.C. Yang¹, D.L. Yu¹, K. Zhang¹, X.R. Duan¹, and HL-2A team

1. *Southwestern Institute of Physics, Chengdu 610041, People's Republic of China*

2. *CEA, IRFM, F-13108 Saint-Paul-lez-Durance, France*

3. *Institute for Fusion Theory and Simulation, Zhejiang University, Hangzhou, 310027, People's Republic of China*

4. *Dalian University of Technology, Dalian 116024, People's Republic of China*

Controlling the enormous heat flux released by large ELMs is a crucial issue for tokamak fusion research. Several techniques have been developed for ELM control, such as resonant magnetic perturbation (RMP) [1], pellet pacing [2], supersonic molecule beam injection (SMBI) [3], lower hybrid current drive (LHCD) [4], and impurity seeding [5]. A group of Evidence has been found that turbulence may play an important role during the control of the ELMs. The ELM mitigation experiments with RMP in MAST [6] and DIII-D [7] suggest that a new turbulence drive mechanism may be crucial to the resulting enhanced transport respecting that the turbulence increases faster than the drive terms evolves. Besides, the turbulence enhancement has been observed in the experimental study of the ELM mitigation on HL-2A with SMBI, LHCD, and impurity seeding [3-6].

In the present experiments in the HL-2A tokamak, the plasma parameters are: major radius $R = 1.65\text{m}$, minor radius $a = 0.4\text{m}$, the toroidal magnetic field $B_0 = 1.3\text{T}$, the plasma current $I_p = 160\text{kA}$, the plasma line averaged density $n_e = 1.8\text{--}2.5 \times 10^{19} \text{ m}^{-3}$. The auxiliary heating power for neutron beam injection is $P_{\text{NBI}} = 1\text{MW}$.

It should be noted that if the diameter of the laser spot is used to indicate the quantity of the impurity, even the same diameter would leads to different effect on ELMs. Thus, in this work the radiation induced by the impurity is used to indicated the quantity of the seeded impurity. To take the impurity transport into consideration, the time averaged radiation power density $\overline{P_{\text{max}}}_{t_1}^{t_2}$ is used to indicate the quantity of the seeded impurity. Here t_1 is the time when the radiation power density starts to change due to LBO impurity seeding. t_2 is the time when the ELM mitigation or suppression ends. Fig.1 shows the effect of impurity density on the ELMs. The variation of the ELMs is presented by the ratio of the D_α signal before and after LBO in y axis. If the ratio is close to 1, the ELMs are not affected by impurity. It should be

noted that there is no ELM during ELM suppression case, thus the averaged value of the D_α during this phase would be used to calculate the ratio. The statistic results of LBO aluminum (Al) impurity with similar plasma density are shown in Fig.1(a). The black solid circles show the no effect cases whose ratio of the D_α signal before and after LBO is about 1 and radiation power density is less than $20(\overline{P_{max}}_{t1}^{t2} \leq 20)$. The blue solid squares give the mitigation cases where the radiation power density locates in a certain area ($20 \leq \overline{P_{max}}_{t1}^{t2} \leq 40$) and the ratio locate between 0.3-0.8. The red solid triangles represent the suppression cases with the value of radiation power density exceeding 40. Similarly, the statistic results of LBO Fe impurity seeding is shown in Fig.1(g). To normalize the data from different species of impurities, a coefficient is applied to the radiation power density induced by iron (Fe). This coefficient is chosen as atomic number Z of the impurities. The statistic results of Al and Fe impurity seeding are shown in Fig.1(c). It could be observed that the thresholds for ELM mitigation and ELM suppression exist, which are $P_{mitig} = 1.8$ and $P_{suppr} = 3$.

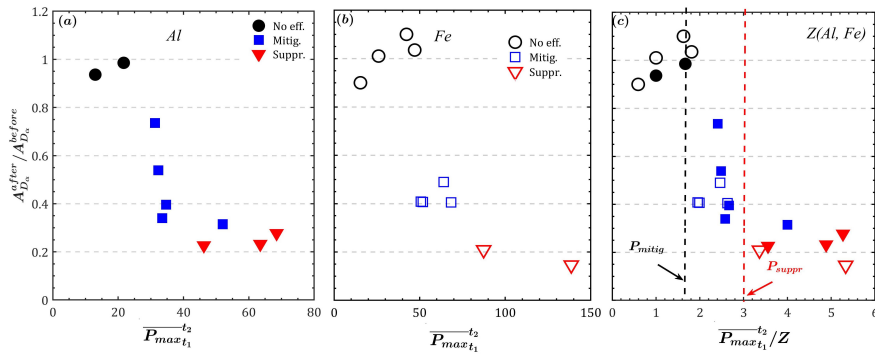


FIG. 1. (color online). The radiation power density versus the D_α ratio after and before LBO. The statistic of the Al impurity discharges(a), The statistic of the Fe impurity discharges(b),The statistic of both Al and Fe impurity discharges(c).

Further analysis on pedestal parameters and turbulence shows that the impurities reduce the velocity shear rate by changing the toroidal velocity term rather than by changing the pressure gradient term as observed in ELM mitigation with LHCD. The reduction of the $E \times B$ velocity shear rate enhances the pedestal turbulence through the turbulence spectral shift process during ELM mitigation as shown in Fig.2(a)-(d). In addition, simulation result of the pedestal turbulence based on the spectral shift model is shown in Fig.2(e)-(h). Similarly, the effect of the impurity on the velocity shear rate is simply treated as a constant value, as shown in Fig.2(e) and Fig.2(f). Meanwhile the averaged radial wavenumber starts to increase with a time delay after the external source input as shown in the experiment in Fig.6(c) and in Fig.2(g). In Fig.2(d) and Fig.2(h), a significant change of the amplitude of the turbulence has

been observed due to the radial wavenumber spectral shift with a longer time delay. Good agreement has been found between the experimental result and the simulation result for the pedestal turbulence behavior during ELM mitigation.

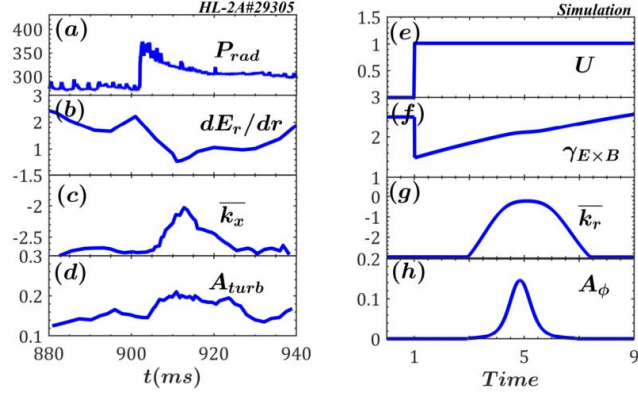


FIG. 2. (color online). The time trace of the experiment data: radiation power from bolometer(a),the E r shear rate(b),the spectral averaged radial wavenumber(c) and the turbulence amplitude(d). The time trace of the simulation data: the reduction value of the velocity shear rate due to LBO(e),the $E \times B$ velocity shear rate(f), the spectral averaged radial wavenumber(g),the turbulence amplitude(h).

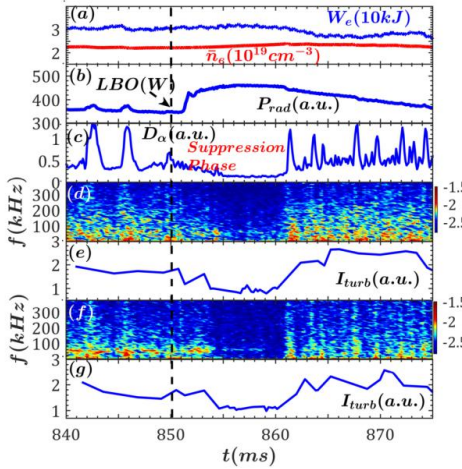


FIG. 3. (color online). The time trace of the averaged electron density(red line) and the plasma stored energy(blue line)(a),the radiation power from the bolometer(b), the D_α signal(c),the turbulence spectrum at the pedestal top(d), the turbulence intensity at the pedestal top(e), the turbulence spectrum at the pedestal bottom(f), and the turbulence intensity at the pedestal bottom(g).

It should be again pointed out that impurity could also reduce the intensity of the turbulence due to the dilution effect when the impurity density is enough. Fig.3 shows the reduction of the turbulence intensity during the ELM suppression phase. At 850ms, the W impurity is injected and after a short time the radiation power starts to increase as shown in Fig.3(b). At the same time, the plasma density and the plasma stored energy slightly increase as shown in Fig.3(a). ELMs are suppressed as shown in Fig.3(c). During the ELM suppression phase, the turbulence spectrum measured by the multi-channel Doppler

reflectometry at the position near the pedestal top and pedestal bottom is shown in Fig.3(c) and Fig.3(f) separately. From the turbulence spectrum, it could be observed that the turbulence reduces during the ELM suppression phase. This could be also observed on the turbulence intensity from these two corresponding Doppler reflectometry channels shown in Fig.3(d) and Fig.3(e).

In conclusion, ELM control has been achieved with different species of the impurities. It has been found that two thresholds of the impurity density exist for ELM control in the normalized statistic result. Besides, the dual effect of the LBO impurity seeding have been found on the pedestal turbulence, which are due to different mechanisms. On one hand, the LBO impurity seeding reduces the $E \times B$ velocity shear rate by changing the ion toroidal velocity term. This is different from the observations with LHCD, where the reduction of the $E \times B$ velocity shear rate attributes to the reduction of the ion diamagnetic term. It should be pointed out that the ion toroidal velocity as well as its gradient becomes larger after LBO while the collision rate is increasing. The reduction of the $E \times B$ velocity shear rate enhances the turbulence intensity through radial wavenumber spectral shift without the change of the correlation length of the turbulence. Good agreements have been found between the experimental observation and simulation result on the turbulence behavior. On the other hand, the LBO impurity seeding reduces the turbulence intensity by decreasing the instability growth rate due to the dilution effect of the main particles in plasma.

REFERENCES

- [1] T.E. Evan et al., *Nature Physics* 2, 419 (2006)
- [2] P.T. Lang et al., *Nucl. Fusion* 43, 1110 (2003)
- [3] W.W. Xiao et al., *Nucl. Fusion* 52, 114027 (2012)
- [4] G.L. Xiao et al., *Phys. Plasmas* 24, 122507 (2017)
- [5] Y.P. Zhang et al., *Nucl. Fusion* 58, 046018 (2018)
- [6] W.L. Zhong et al., *Nucl. Fusion* 59, 076033 (2019)
- [7] A. Kirk et al., *Nucl. Fusion* 50, 034008 (2010)
- [8] G.R. McKee et al., *Nucl. Fusion* 53, 113011(2013)